

AD-A101 656

JOINT INST FOR LAB ASTROPHYSICS BOULDER CO
MULTI-TERM BOLTZMANN ANALYSIS OF ELECTRONS IN N2. (U)

F/G 7/4

MAY 81 L C PITCHFORD, A V PHELPS

MIPR-FY1455-80-00608

UNCLASSIFIED

AFWAL-TR-81-2035

NL

1 of 1
AD-A
CIC1856

END
FILED
8-81
DTIC

AD A101656

AFWAL-TR-81-2035

LEVEL 12

12



MULTI-TERM BOLTZMANN ANALYSIS OF ELECTRONS IN N₂

L.C. PITCHFORD, A.V. PHELPS

JOINT INSTITUTE FOR LABORATORY ASTROPHYSICS
UNIVERSITY OF COLORADO AND NATIONAL BUREAU OF STANDARDS
BOULDER, CO 80309

MAY 1981

FINAL REPORT FOR PERIOD OCTOBER 1 1979 THROUGH SEPTEMBER 30 1980



DTIC FILE COPY

Approved for public release; distribution unlimited.

AERO PROPULSION LABORATORY
AIR FORCE WRIGHT AERONAUTICAL LABORATORIES
AIR FORCE SYSTEMS COMMAND
WRIGHT-PATTERSON AIR FORCE BASE, OHIO 45433

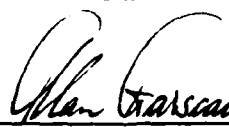
81 7 21 013

NOTICE

When Government drawings, specifications, or other data are used for any purpose other than in connection with a definitely related Government procurement operation, the United States Government thereby incurs no responsibility nor any obligation whatsoever; and the fact that the government may have formulated, furnished, or in any way supplied the said drawings, specifications, or other data, is not to be regarded by implication or otherwise as in any manner licensing the holder or any other person or corporation, or conveying any rights or permission to manufacture use, or sell any patented invention that may in any way be related thereto.

This report has been reviewed by the Office of Public Affairs (ASD/PA) and is releasable to the National Technical Information Service (NTIS). At NTIS, it will be available to the general public, including foreign nations.

This technical report has been reviewed and is approved for publication.


Alan Truscadden.
PROJECT ENGINEER


Robert R. Bartholemey
ROBERT R. BARTHELEMY
Chief, Energy Conversion Branch
Aerospace Power Division
Aero Propulsion Laboratory

FOR THE COMMANDER


J D Reams
JAMES D. REAMS
Chief, Aerospace Power Division
Aero Propulsion Laboratory

"If your address has changed, if you wish to be removed from our mailing list, or if the addressee is no longer employed by your organization please notify POOC-3, W-PAFB, OH 45433 to help us maintain a current mailing list".

Copies of this report should not be returned unless return is required by security considerations, contractual obligations, or notice on a specific document.

of boundaries by comparing the Boltzmann results with Monte Carlo studies in nitrogen at moderate field strengths. These calculations were done using a set of cross-sections previously derived from swarm experiments and the fields were constrained to be low enough that secondary electrons resulting from ionization were safely ignored. The extension of the calculations to higher fields was accomplished by using higher energy cross-sections than available from the swarm data and by slight modification of the computational techniques. The effect of anisotropic scattering was investigated and found to be negligible at low field strengths but quite important at the one higher field of 500 Townsends that was investigated. Calculations are presented for field strengths high enough that 50% of the electron energy loss is to ionization. Implications of these results are discussed.

Accession For	<input checked="" type="checkbox"/>
NTIS GRAF	<input type="checkbox"/>
DTIC TAB	<input type="checkbox"/>
Unannounced	<input type="checkbox"/>
Justification	<hr/>
By	<hr/>
Distribution/	<hr/>
Availability Codes	<hr/>
DIS	<hr/>
A	

PREFACE

This work was performed at the Joint Institute for Laboratory Astrophysics under contract number MIPR FY1455 80-00608, during the period October 1979 through September 1980.

The authors would like to acknowledge a computer grant from the National Center for Atmospheric Research, Boulder, Colorado. The final calculations at the high field strengths were supported in part by the U.S. Army Research Office under MIPR No. ARO 9-81 and are included in this report in order to complete the technical presentation. The Air Force project engineer was Dr. Alan Garscadden, Energy Conversion Branch, Aerospace Power Division of the Aero Propulsion Laboratory.

TABLE OF CONTENTS

<u>Section</u>	<u>Page</u>
I. INTRODUCTION	1
II. MATHEMATICAL MODEL AND SOLUTION METHOD	3
III. MODERATE FIELD STRENGTHS	8
1. Convergence of the Distribution Function and Transport Parameters	10
2. Boundary Effects	18
IV. HIGH FIELD STRENGTHS	21
1. Differential Scattering Cross Sections in N_2	21
2. Boltzmann Treatment of Ionization	22
3. Numerical Results Considering Ionization	25
4. Anisotropic Scattering Effects	28
V. CONCLUSIONS	32
REFERENCES	35

LIST OF ILLUSTRATIONS

<u>Figure</u>	<u>Page</u>
1 Electron Collision Cross Section for N_2	9
2 Electron Energy Distribution for N_2	11
3 f_0 in N_2 at $E/N = 10^{-15} \text{ V cm}^2 = 100 \text{ Td}$	12
4 Convergence of Transport and Excitation Coefficients for N_2 at $E/N = 10^{-15} \text{ V-cm}^2 = 100 \text{ Td}$	14
5 Errors Due to 2-Term Solution of Boltzmann Equation for N_2	15
6 Error in Transverse Diffusion Coefficient	17
7 Monte Carlo Calculation of Excitation for $[N_2] = 10^{17} \text{ cm}^{-3}$ at $EN = 10^{-15} \text{ V-cm}^2 = 100 \text{ Td}$	19

LIST OF TABLES

<u>Table</u>		<u>Page</u>
1	Ratios of Spherical Harmonic Components of Cross Sections in N ₂	23
2	The Effect of Electron Production During Ionization	27
3	Anisotropic Scattering and Ionization at 500 Td	30

SECTION I

INTRODUCTION

The macroscopic properties of a low density cloud or swarm of electrons in a neutral gas under the influence of an electric field can be calculated from solutions of the Boltzmann equation or with Monte Carlo techniques if the appropriate cross sections are provided. Information on such properties is critical to the understanding of phenomena in gaseous electronics. When the cross sections are uncertain, comparisons of calculated swarm parameters with measurements using estimates for the cross sections can lead to refined estimates for these cross sections. Some of the best estimates of the low (thermal to several volts) energy electron scattering cross sections from atoms and simple molecules have been derived from such techniques.¹ The accuracy of the calculated swarm parameters or the cross sections so derived depends on the accurate solution of the Boltzmann equation.

Many approaches have been used for the numerical solution of the Boltzmann equation for equations in the context of swarms.² By far the most common method is the two-term expansion solution; the electron velocity distribution function is expanded in spherical harmonics and the expansion is truncated after the first two terms.³ Computer codes to implement this technique have been developed and widely circulated,⁴ especially throughout the laser community.

Last year, under this contract, a multi-term spherical harmonic expansion method was developed⁵ which is especially suited for implementation on the large-scale vector computers becoming available now. Here we use that method to investigate the validity of the two-term approximation in N₂. We have also used the multi-term method to study the effects of ionization and anisotropic scattering cross sections.

In Section II, we outline the multi-term method. A detailed description can be found in the final report from 1979.⁶ In Section III, we present studies of the convergence of the swarm parameters using the Boltzmann code and the effect of boundaries by comparing the Boltzmann results with Monte Carlo studies in N₂ at moderate field strengths. The calculations in that section were done using a set of cross sections previously derived from swarm experiments⁷ and the fields were constrained to be low enough that secondary electrons resulting from ionization were safely ignored. The extension of the calculations to higher fields required values of higher energy cross sections than were available in the swarm derived data set and slight modifications of the calculational techniques. The effect of anisotropic scattering was investigated and found to be negligible at low field strengths but quite important at the one example shown for higher fields. These items are discussed in Section IV and we present calculations up to field strengths high enough that about 50% of the electron energy loss is to ionization.

The implications of this work are discussed in Section V.

SECTION II

MATHEMATICAL MODEL AND SOLUTION METHOD

The Boltzmann equation for electrons defines the electron energy distribution function, $f(\vec{r}, \vec{v}, t)$ and is written as,

$$\frac{\partial f}{\partial t} + \vec{v} \cdot \vec{\nabla}_r f + \vec{a} \cdot \vec{\nabla}_v f = C(f) \quad (1)$$

where \vec{a} is the acceleration due to an external electric field and C is the collision operator. Since Eq. (1) depends on three variables, \vec{r} , \vec{v} , and t , some assumptions must obviously be made in order to solve for f . In the regime of drift tube experiments, the usual assumptions^{2a,b} are

$$\frac{\partial f}{\partial t} = 0 \quad (2a)$$

and

$$\vec{\nabla}_r f = 0 \quad . \quad (2b)$$

These two assumptions reduce the dependence of f from seven variables to the three velocity variables. At this point a further assumption is usually made, namely, that the angular dependence of $f(\vec{v})$ can be approximated by the first two terms of a spherical harmonics expansion, or rather Legendre expansion because of the cylindrical symmetry,

$$f(\vec{v}) = f(\epsilon, \theta) = f_0(\epsilon) + f_1(\epsilon) \cos \theta \quad . \quad (2c)$$

The first assumption [Eq. (2a)] is met satisfactorily in the drift tube experiments when field strengths are low enough that there is no appreciable ionization and where there is no attachment. Then the electrons do reach an equilibrium fairly quickly on the time scale of the experiments. The second assumption [Eq. (2b)] is also fairly accurate in these cases, but in order to

calculate diffusion coefficients, it is necessary to include the effect of the spatial gradients in some way. Parker and Lowke⁸ and Skullderud,⁹ for example, have proposed methods for doing this. The third assumption [Eq. (2c)] is the "two-term" approximation. In order for the two-term assumption to be valid, the inelastic cross sections must be small compared to the elastic cross sections,^{3a} i.e., on the average the electrons must lose only a small fraction of their initial energy upon colliding with the neutral gas atoms or molecules. This is not always the case, especially for molecules. Implicit in the two-term approximation, but not usually stated, is the idea that the electron-neutral cross sections are no more anisotropic than $\cos \theta$. In other words, if the cross sections were also expanded in spherical harmonics, it would only be the first two terms that would enter into the calculation.

The method we use to solve the Boltzmann equation have been described in detail previously^{5,6} for the case of no ionization. We will summarize the method here and address the extension to the case where ionization is present. We include the t and \vec{r} dependence of the distribution following the method proposed by Skullderud⁹ in which the full distribution function, including the \vec{r} and t dependence, is expanded in powers of the spatial gradient of the electron density, $n(\vec{r}, t)$;

$$f(\vec{r}, \vec{v}, t) = f^{(0)}(\vec{v})n(\vec{r}, t) - \vec{f}^{(1)}(\vec{v}) \cdot \vec{\nabla}n(\vec{r}, t) + \sum_{k=2} \underline{f}^{(k)}(\vec{v}) \times (-\vec{\nabla})^{(k)}n(\vec{r}, t) \quad . \quad (3)$$

The first term in this expansion is the simple product of a velocity distribution function and a density distribution function. The succeeding terms can be thought of as corrections to this simple product approximation.

Combining this expansion with the Boltzmann equation we write,

$$\begin{aligned}
 f^{(0)}(\vec{v}) \frac{\partial n(\vec{r}, t)}{\partial t} - \vec{f}^{(1)}(\vec{v}) \cdot \vec{\nabla} \frac{\partial n(\vec{r}, t)}{\partial t} \\
 + \vec{a} \cdot \vec{\nabla}_{\vec{v}} f^{(0)}(\vec{v}) n(\vec{r}, t) - \vec{a} \cdot \vec{\nabla}_{\vec{v}} \{ \vec{f}^{(1)}(\vec{v}) \cdot \vec{\nabla} n(\vec{r}, t) \} \\
 + \vec{v}^{(0)} \vec{v} \cdot \vec{\nabla}_{\vec{r}} n(\vec{r}, t) - \vec{v} \cdot \vec{\nabla}_{\vec{r}} \{ \vec{f}^{(1)}(\vec{v}) \cdot \vec{\nabla} n(\vec{r}, t) \} + \dots \\
 = C \{ f^{(0)}(\vec{v}) n(\vec{r}, t) - \vec{f}^{(1)} \cdot \vec{\nabla} n(\vec{r}, t) \} + \dots . \quad (4)
 \end{aligned}$$

The continuity equation for electrons provides an expression for the time derivative in the first two terms,

$$\frac{\partial n(\vec{r}, t)}{\partial t} = \omega^{(0)} n(\vec{r}, t) - \vec{v}^{(1)} \cdot \vec{\nabla} n(\vec{r}, t) + \underline{\omega}^{(2)} : \vec{\nabla} \vec{\nabla} n(\vec{r}, t) \quad (5)$$

where the $\omega^{(0)}$ is the electron gain frequency due to ionization, $\vec{v}^{(1)}$ is the drift velocity, $\underline{\omega}^{(2)}$ is the diffusion tensor, and the succeeding ω 's are higher order transport coefficients.

Combining Eqs. (4) and (5),

$$\begin{aligned}
 [-\omega^{(0)} f^{(0)} + \vec{a} \cdot \vec{\nabla}_{\vec{v}} f^{(0)} - C(f^{(0)})] n \\
 + [-\omega^{(0)} \vec{f}^{(1)} + \vec{a} \cdot \vec{\nabla}_{\vec{v}} \vec{f}^{(1)} - C(\vec{f}^{(1)})] \cdot \vec{\nabla} n + (\vec{v} - \vec{v}^{(1)}) f^{(0)} \cdot \vec{\nabla} n \\
 + \dots = 0 . \quad (6)
 \end{aligned}$$

A hierarchy of equations results from setting coefficients of powers of the gradient of n equal to zero. The first two equations are,

$$\vec{a} \cdot \vec{\nabla}_{\vec{v}} f^{(0)}(\vec{v}) - \omega^{(0)} f^{(0)} - C(f^{(0)}) = 0 \quad (7a)$$

$$\vec{a} \cdot \vec{\nabla}_{\vec{v}} \vec{f}^{(1)}(\vec{v}) - \omega^{(0)} \vec{f}^{(1)} - C(\vec{f}^{(1)}) = -(\vec{v} - \vec{v}^{(1)}) f^{(0)} \quad (7b)$$

and the ω 's for $k > 0$ can be written as

$$\underline{\omega}^{(k)} = \int \underline{v} \underline{f}^{(k-1)} \underline{d}^3 v . \quad (8)$$

These equations can be solved in order, first for $f^{(0)}$, then for the higher order terms. Thus, the effect of spatial and temporal gradients are treated as exactly as necessary for the ω 's of interest. The only iteration required is in the determination of $\omega^{(0)}$ in the first equation and we return to this point later. The problem is now reduced to solving the first equation, (7a). The same method may then be applied to the second and succeeding equations if those are desired.

The method described below is shown for $f^{(0)}(\underline{v})$, but the same methods have been applied to the calculation of $\underline{f}^{(1)}(\underline{v})$. We first expand the distribution function in spherical harmonics, or rather Legendre functions, because of the cylindrical symmetry,

$$f^{(0)}(\underline{v}) \equiv f(\epsilon, \theta) = \sum_i^N f_i(\epsilon) P_i(\cos \theta) . \quad (9)$$

However, rather than considering only two terms, we retain an arbitrary number of terms at this point. The substitution of the spherical harmonic expansion into the Boltzmann equation results in a set of coupled differential equations for the coefficients, $f_i(v)$. The complication in solving these equations comes from the nonlocal nature of the collision terms due to the inelastic and superelastic collisions. When a simple two-term expansion is used, the resulting set of coupled differential equations may be combined into one second-order differential equation for $f_0(v)$ which is often solved by the "backward prolongation"¹⁰ technique. Rather than attempt to extend the backward prolongation idea to the coupled system, we have used a global approach.

In order to implement a global solution, the coefficients, $f_i(\epsilon)$, are further expanded in some set of known functions, cubic B-splines, $S(\epsilon)$.¹¹

In our case,

$$f_i(\epsilon) = \sum_{j=1}^{N_s} C_{ij} S_j(\epsilon) + \delta_i \quad . \quad (10)$$

Since the splines do not form a complete set because we do not consider an infinite number of them, there is a small error term, δ_i , in the expansion. The error can be forced equal to zero at each point on a set of grid points spanning the velocity range of interest by requiring $\langle S_j(\epsilon) | \delta_i \rangle = 0^{12}$ for $i = 0, 1, 2, \dots, N_d$ and $j = 1, 2, \dots, N_s$. This allows us to write the set of coupled differential equations in the form of a system of linear algebraic equations which can be expressed as a matrix equation, $MC = B$, where the M 's are functions of the cross sections, E/N , and velocity. The elements of B contain the boundary conditions. This equation can be easily solved by any of a number of matrix inversion methods to yield the desired coefficients, the C 's. Given the C 's, we can construct the $f_i(\epsilon)$'s and, hence, the total distribution function.

For the calculations reported here, we used typically 100 splines to cover the energy range. The energy range was from zero to the point where the distribution function had dropped five to seven orders of magnitude from its peak. The grid defining the splines was unevenly spaced for maximum flexibility and the integrals were performed with range-splitting Gauss-Legendre quadrature techniques. All the nonphysical parameters were varied to ensure that the final solution depended in no way on the high energy cut-off or number of splines.

SECTION III

MODERATE FIELD STRENGTHS

In this section, we discuss the convergence of the distribution function and transport and rate coefficients calculated using the method discussed in Section II in the case of N_2 over a range of E/N from 1 to 200 Td and show comparisons of the two-term, multiterm and Monte Carlo results. Our expectation is that these results are very typical of other molecular gases which have similar electron scattering cross sections.

In this range of E/N in N_2 average electron energies go from well below the onset of the vibrational thresholds, through the vibrational maximum, and fall slightly short of the onset of the electronic thresholds. The cross section set⁷ used for these calculations is shown in Figure 1. These cross sections are isotropic. The momentum transfer cross sections shown in the figure is the total momentum transfer, the sum of the elastic and inelastic momentum transfer cross sections. The rotational excitation cross sections, for which an example is shown in Figure 1, were replaced by a single level cross section. The vibrational and electronic cross sections are shown in the figure as sums of the individual level excitations. In the calculation we considered the individual level cross sections and, with ionization, a total of 23 inelastic cross sections were included. We restrict ourselves here to the range of E/N low enough that ionization may be treated as an energy loss mechanism. At the highest value of E/N considered, 200 Td, about 3% of the electronic energy lost goes into ionization. For higher E/N , the electrons born in the ionization events begin to significantly affect the distribution and must be included as will be discussed.

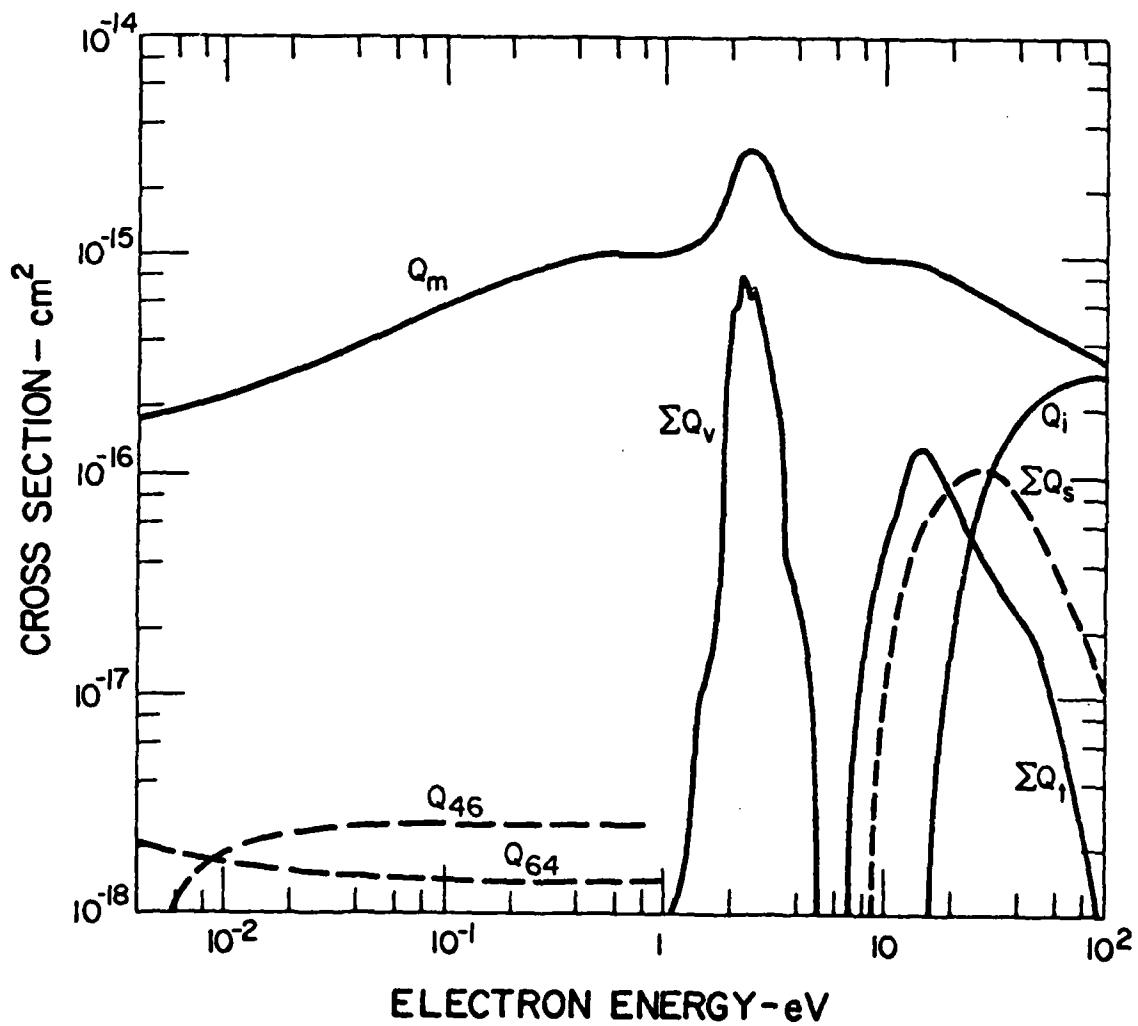


Figure 1. Electron collision cross section for N_2 . N_2 cross sections used in the calculations of Section III. Excitation cross sections are shown as sums over many levels. In the calculations, all of the 23 individual cross sections were used rather than the sums.

1. Convergence of the Distribution Function and Transport Parameters

Since the computational problem is the determination of the spherical harmonic expansion coefficients, the f_i 's, we will first look at those. The normalized $f_i(\varepsilon)$'s in N_2 at an E/N of 100 Td (where the average energy of the electrons in the swarm is 2.2 eV) are shown in Figure 2 as a function of energy. The results shown are the first four coefficients in a six-term expansion. The isotropic component, f_0 , is the largest at all energies. The higher order coefficients are smaller but still significant in comparison to f_0 . This is especially true in the 2 eV region where the vibrational cross sections are large. The considerable structure in the 2 eV region and again around 7-8 eV seems to reflect the onset of important inelastic cross sections at those energies. As will be seen later, the f_0 component of the distribution function calculated from only two-terms in the case shown may be quite different from the multiterm result.

However, only the first few coefficients enter into the calculation of the measurable parameters of interest in most swarm applications and not the total distribution function. For the calculation of those measurables, it is really not important to have the full distribution function. The important thing here is to determine how well we have calculated the first few coefficients. Due to the coupling in the equations, the solution obtained for f_0 , for example, will depend on the number of terms in the expansion. Figure 3 shows a comparison of f_0 calculated from a two-term approximation, a six-term approximation, and a Monte Carlo technique.¹³ This is the same case as seen in Figure 2, N_2 at 100 Td. The six-term and Monte Carlo values of f_0 compare very well at all energies except those around the origin. Since these are two completely different methods, the conclusion drawn from this is that f_0 converges very quickly as a function close to the correct solution even though the

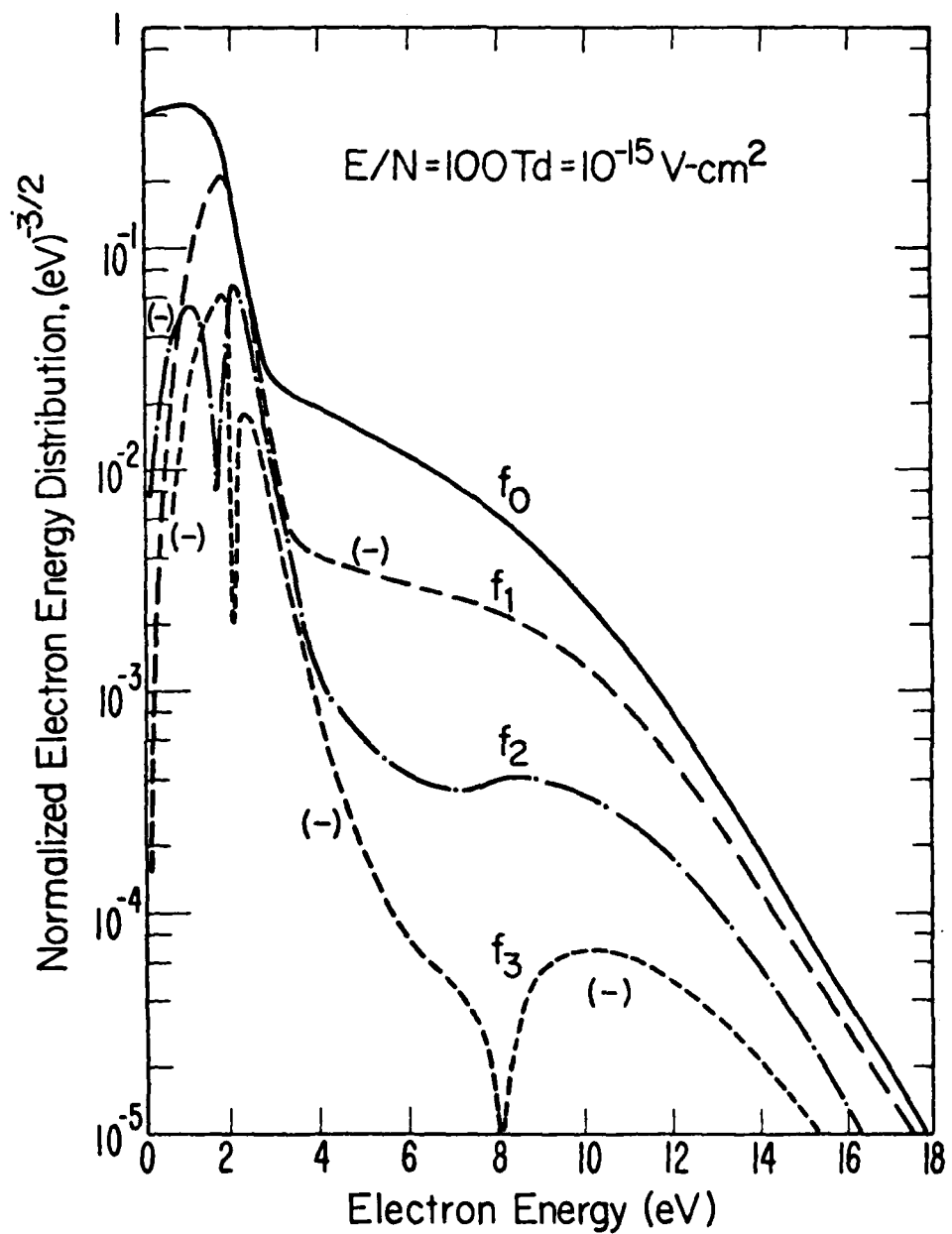


Figure 2. Electron energy distribution for N_2 . The first four normalized Legendre coefficients of the distribution function in N_2 at 100 Td in a six-term calculation.

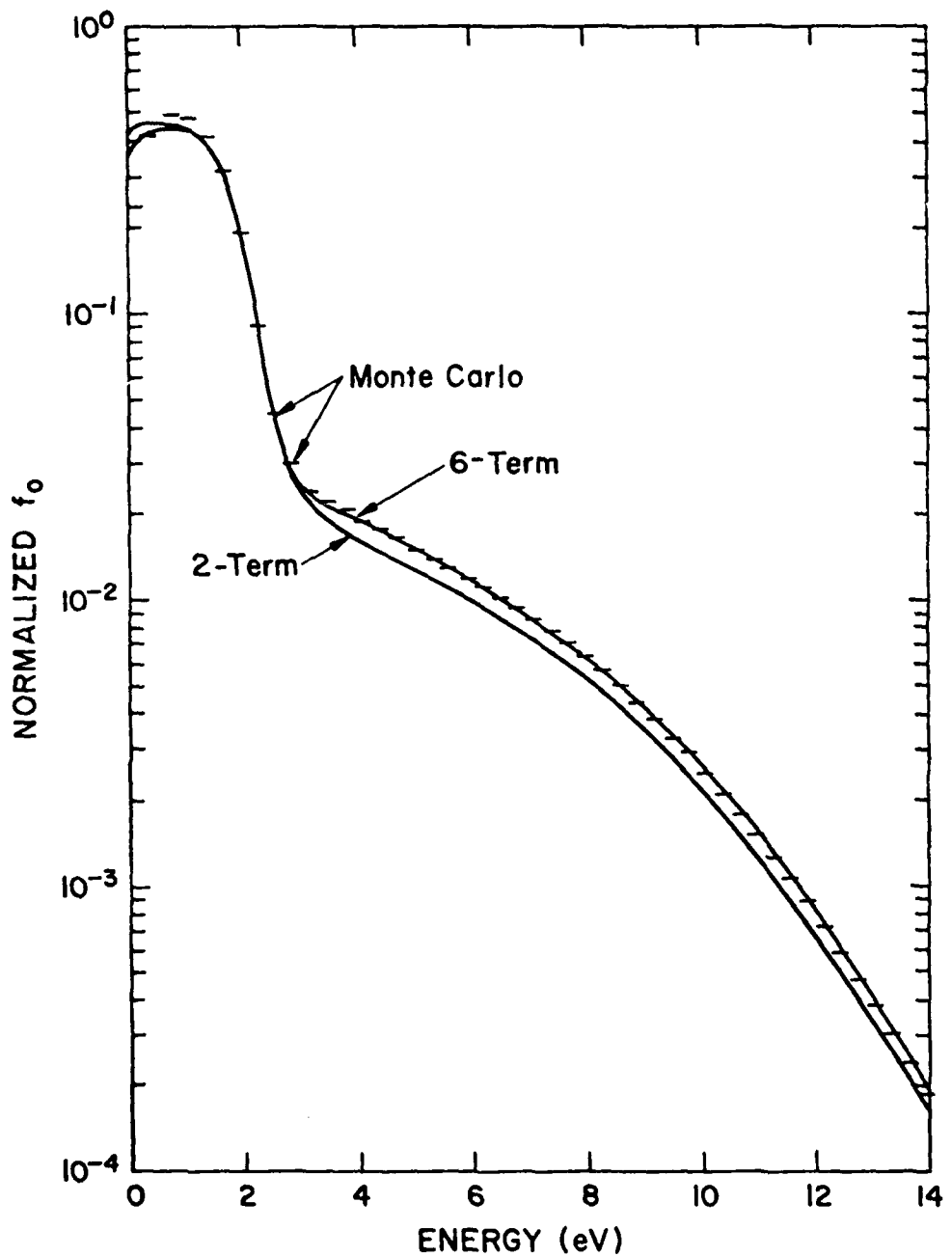


Figure 3. f_0 in N_2 at $E/N = 10^{-15} \text{ V cm}^2 = 100 \text{ Td}$. Comparison of the normalized f_0 , the isotropic component of the distribution function, calculated using a two-term and six-term Boltzmann code and a Monte Carlo calculation.

higher order coefficients in Figure 2 are still quite large. A four-term calculation was also done for this case and yielded an f_0 very close to the six-term value indicating independently the convergence of the six-term f_0 .

The convergence of the transport coefficients, drift velocity and diffusion coefficients, and rate coefficients is connected very closely to the convergence of f_0 as can be seen in Eqs. (8) and (9). Figure 4 shows the convergence of the transport coefficients, drift velocity (v_d), transverse and parallel diffusion (D_T and D_p) coefficients and the $A^3\Sigma$ electronic excitation rate in case of nitrogen at 100 Td as a function of the order of the solution or the number of spherical harmonic components used in the calculation. From the figure it can be seen that the two-term values of the drift velocity and the transverse diffusion coefficient are higher than the higher-order calculations. Conversely, the values of the A -state excitation rate, illustrative of electronic excitation in general, and the parallel diffusion coefficient are lower in the two-term than in the higher-order calculations. The calculated values are seen to converge as the order of the calculation is increased.

Beyond four terms, there is very little change in the values.

Calculations similar to the one presented in Figure 4 were carried out over a range of E/N from 1 to 200 Td and the difference between the two-term results and the six-term results are shown in Figure 5 as a function of E/N . The convergence of the parameters shown in Figure 4 for the seven values of E/N investigated is similar to the 100 Td case seen in Figure 3. We consider here the six-term values to be the converged results. As for the 100 Td case, the values of the drift velocity and the transverse diffusion coefficient in the two-term calculation are higher than the converged result. The difference increases with increasing E/N to a maximum and then decreases. Similarly for the $A^3\Sigma$, $C^3\Pi$, and $W^4\Delta$ electronic excitation rates, the difference increases to a point and then

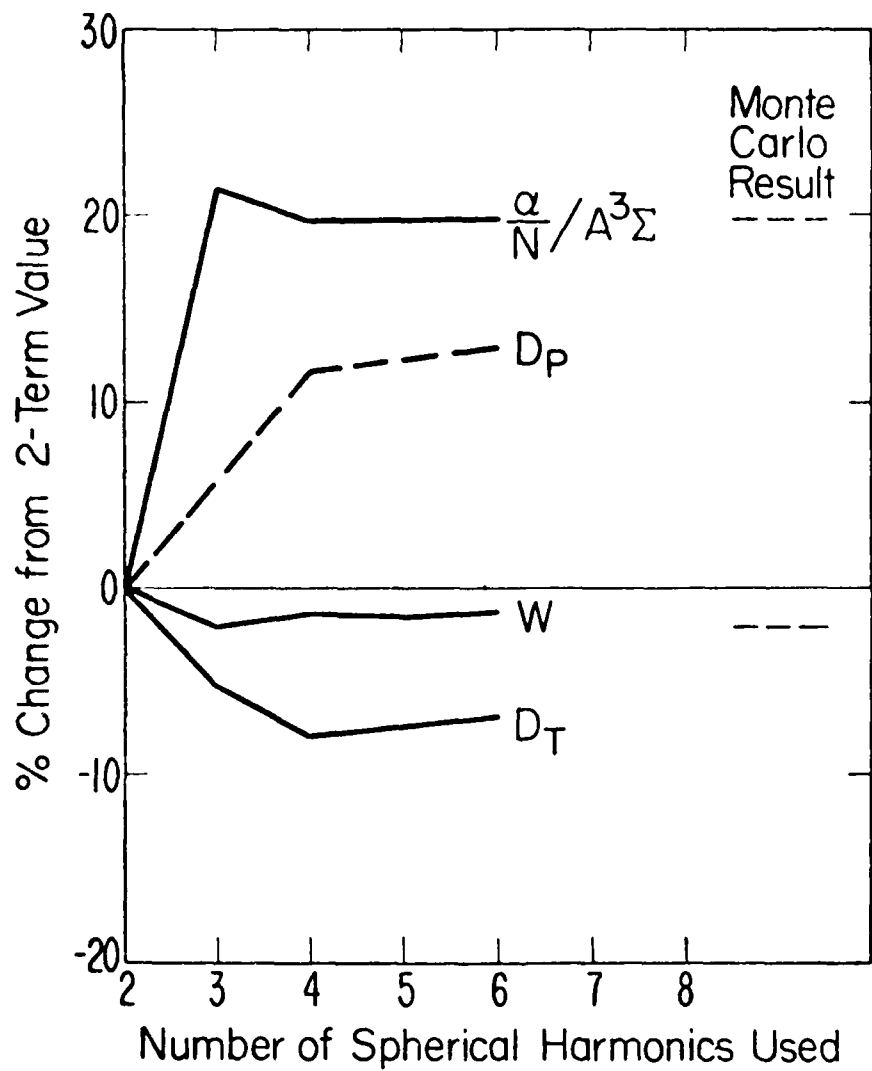


Figure 4. Convergence of transport and excitation coefficients for N_2 at $E/N = 10^{-15} \text{ V-cm}^2 = 100 \text{ Td}$. The convergence as a function of the order of the solution for the drift velocity, transverse and parallel diffusion and A state excitation in N_2 at 100 Td.

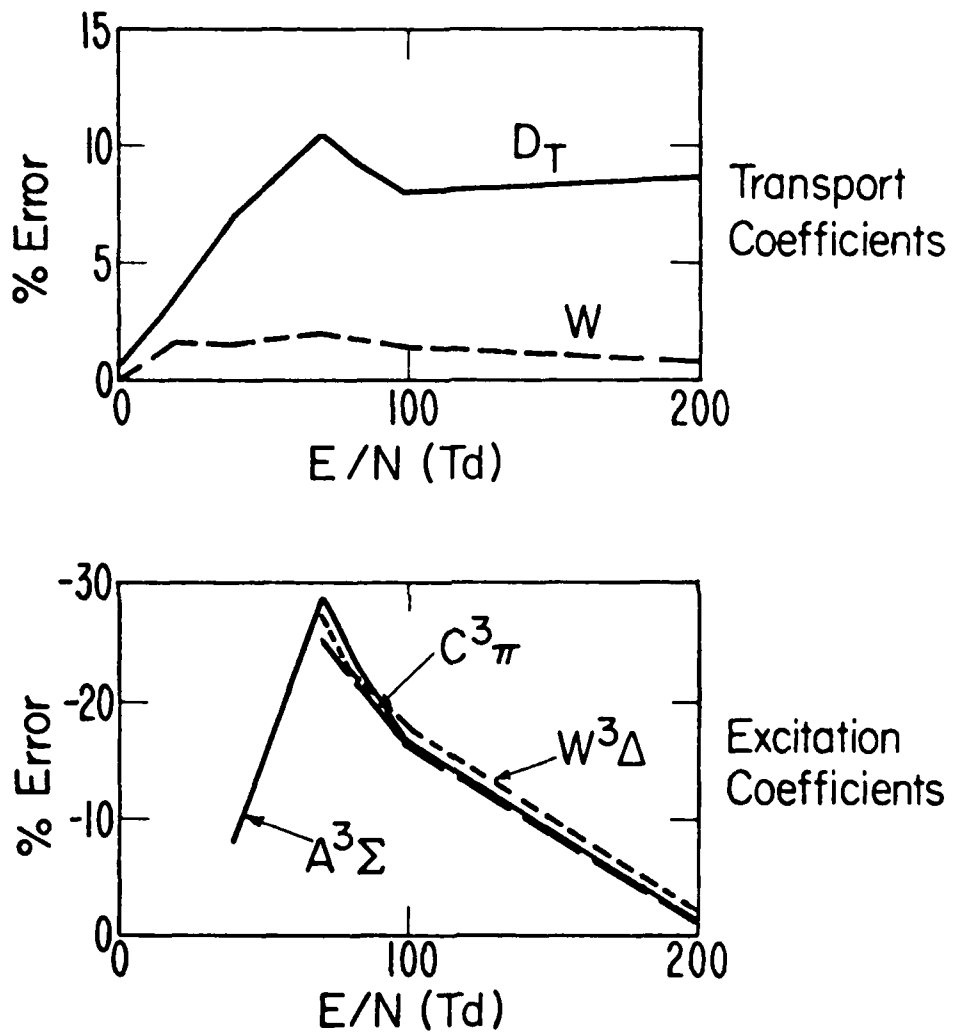
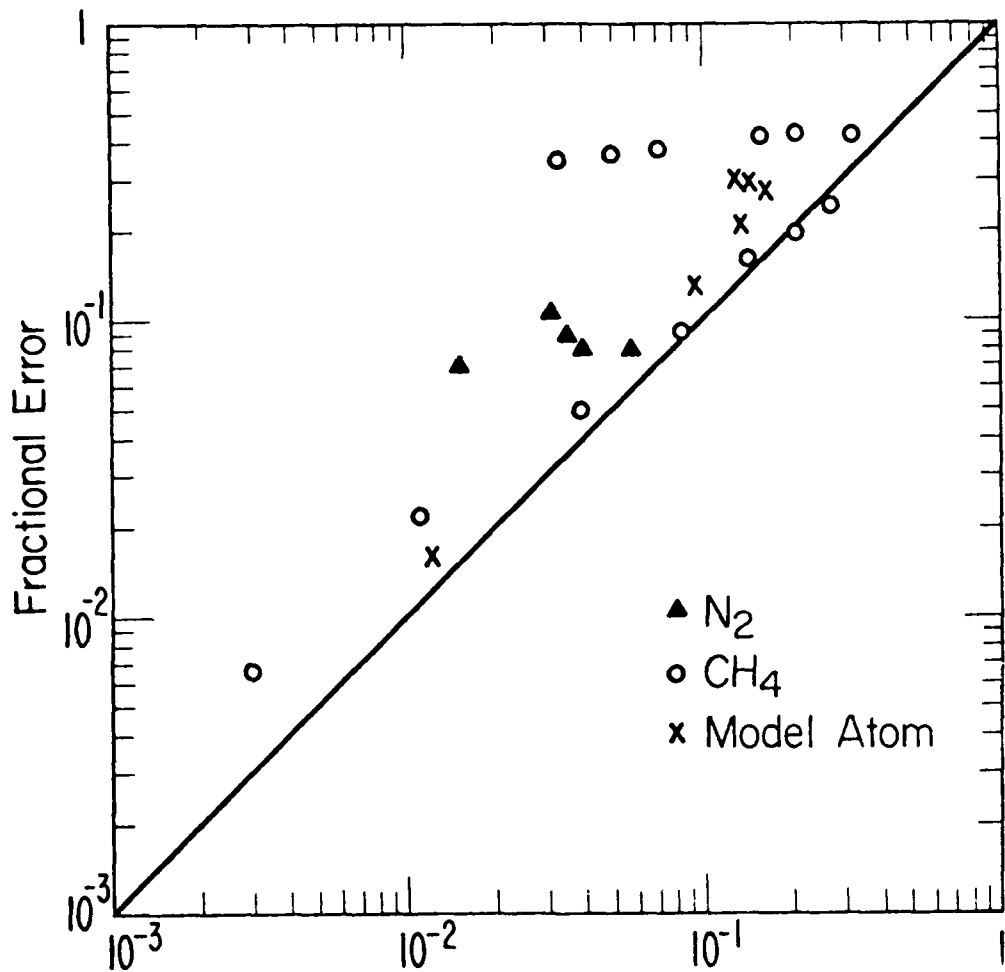


Figure 5. Errors due to 2-term solutions of Boltzmann equation for N_2 . Error introduced by the two-term approximation when compared to the six-term solutions for drift velocity, transverse diffusion, and certain electronic excitation rates as functions of E/N .

decreases, but here the two-term values for the excitation rates are lower in general than the converged results. The maximum difference in each case occurs at 70 Td. At this value of E/N , the power lost by the electrons due to elastic collisions is at a minimum due to the onset of the vibrational cross sections, and based on the criteria of small fractional power lost per collision,^{3a} we would expect the two-term approximation to be worse in this region.

The general trends in extending the order of solution from two to six terms are an elongation in energy of the distribution function as reflected in an increase in the electronic excitation rate and a decrease in the drift velocity and diffusion coefficient. These trends are seen in both Figures 3 and 4. The elongated tail results from a straggling effect;¹⁴ it is only electrons that have avoided collisions that can acquire a relatively high energy from the field. These electrons will have velocities directed almost parallel to the field and the "almost spherical" or two-term approximation will not include these electrons.

Attempts to parametrize the difference between the two-term calculation and the multi-term calculation have been only partially successful. One such attempt is shown in Figure 6, the fractional error in the two-term transverse diffusion coefficient as a function of the ratio of the energy exchange collision frequency to the momentum transfer collision frequency. This ratio is very nearly equal to the ratio of the drift or directed energy to the random energy. When this number is large, the distribution function converges very slowly and we would expect the two-term approximation to introduce significant error. About all that can be said from this plot is that the error always falls above a straight line with a slope of unity. Lin et al.^{3f} also give criteria for the error in the various coefficients due to the two-term approximation. Their equations give a line for this case that falls below ours by about a factor of two.



$$\frac{\text{Energy Exchange Freq.}}{\text{Momentum Exchange Freq.}} = \frac{\nu_u}{\nu_m} \left(\frac{\text{Drift Energy}}{\text{Random Energy}} \right)$$

Figure 6. Error in transverse diffusion coefficient. An attempt to parameterize the two-term error in the transverse diffusion coefficient. The fractional error is plotted as a function of the ratio of the energy exchange frequency to the momentum exchange frequency for three cases, N_2 , a methane model and a model atom.

''. Boundary Effects

In order to compare experimental values of the swarm parameters with those calculated, we must determine how well the mathematical model approximates the experimental situation. Thus far, we have applied the Boltzmann equation to the calculation of swarm parameters and have determined that the approximations are valid and that the solutions are converged. It remains to show that the Boltzmann approach is an appropriate model of the experiments. The Boltzmann approach taken here cannot take into account the effect of the physical boundaries present in experiments. A Monte Carlo simulation was done to access the importance of the boundaries on the calculated values of swarm parameters.

We have performed Monte Carlo calculations in N_2 using the set of cross sections presented in Figure 1. The simulation conditions of a one cm drift distance and a density of 10^{17} cm^{-3} at 100 Td were chosen to approximate the experiments of Tachibana, Levron and Phelps¹⁵ and Urosevic.¹⁶ For this calculation, single electrons were released normal to the cathode with a 2 eV start energy. The electrons were allowed to drift through the tube and were absorbed at the cathode and anode. Upon absorption, a new electron was released with the same start conditions. The simulation continued until the electrons encountered 10^6 collisions with the neutrals. A record was kept after each collision of the type of collision and the position of the electron in the drift tube when the collision took place. From this record we have plotted the number of excitation events per distance interval as a function of distance as seen in Figure 7 for the $v = 0+1$ and $A^3\Sigma$ excitations.

The effect of the cathode and anode can be seen in the figures as a departure from the equilibrium excitation rates. One would expect an energy equilibrium to be established after the distance required for the drift and diffusion currents to become equal or D/W which for this case is about 0.02 cm. This can

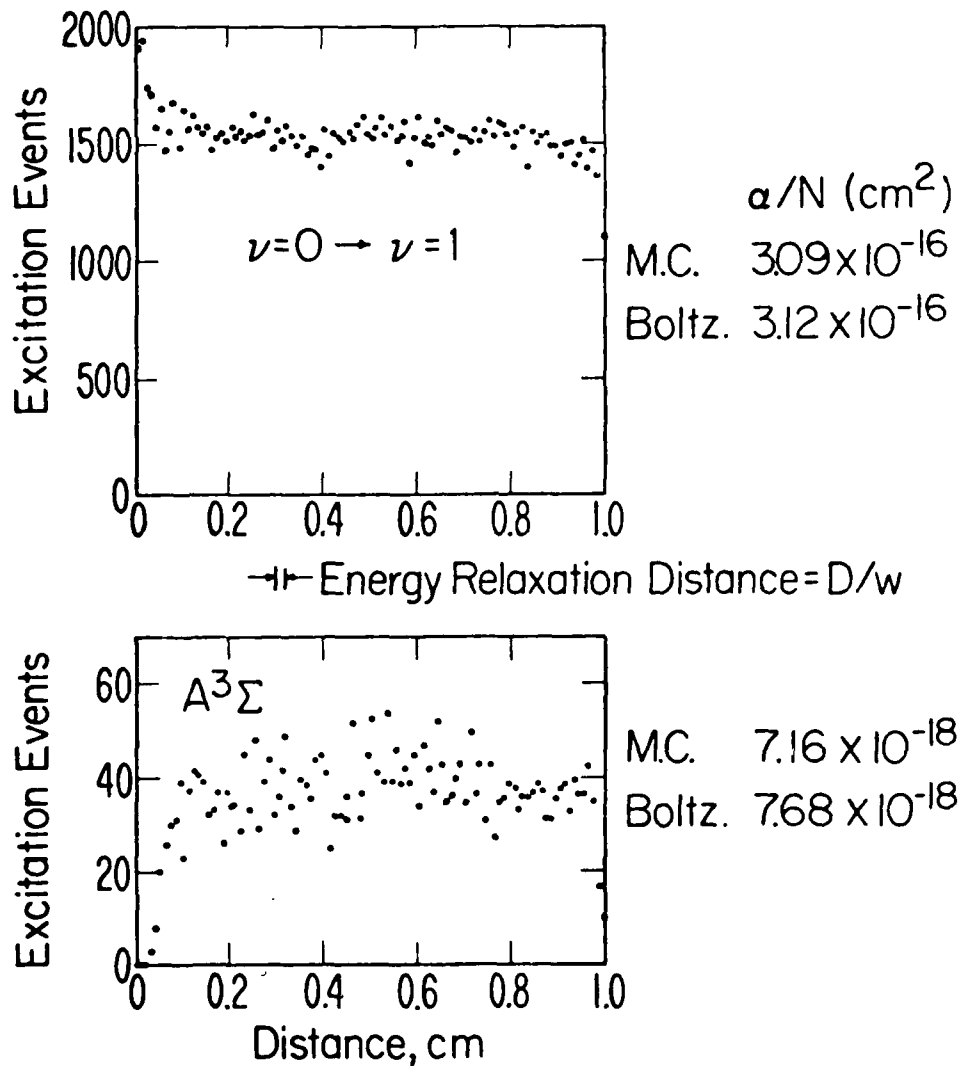


Figure 7. Monte Carlo calculation of excitation for $[N_2] = 10^{17} \text{ cm}^{-3}$ at $E/N = 10^{-15} \text{ V-cm}^2 = 100 \text{ Td}$. Monte Carlo calculations of a number of excitation events as a function of distance in a drift region for the $\nu = 0 \rightarrow 1$ vibrational excitation and $A^3\Sigma$ electronic excitation. Excitation rates may be determined from such data as discussed in the text.

be viewed as the characteristic distance to approach equilibrium or the 1/e distance to equilibrium. This is roughly the distance seen in the figures necessary to reach the equilibrium rates. The $v = 0+1$ excitation starts out higher than the equilibrium because the release energy of 2 eV is equal to the energy at which the vibrational excitation cross section is a maximum. Similarly, the $A^3\Sigma$ state excitation with a threshold energy of 6.17 eV cannot take place until some electrons have gained enough energy from the field to reach the A state threshold. These trends in the excitation near the cathode do, of course, depend on the release energy chosen.

The anode effects are independent of the release conditions provided an equilibrium has been established at some point in the drift region. Here we again see boundary effects on a scale corresponding to the D/W energy relaxation distance. There will be a deficiency of low energy electrons near the anode because of the reduction in the number of backscattered electrons due to absorption of electrons at the anode.

The excitation rates calculated from the Boltzmann code and those from the Monte Carlo simulation are compared on the right of the figures. The agreement is good for the $v = 0+1$ transition and only fair for the A state excitation. However, when excitation events near the boundaries (0.1 cm on either end) are excluded, the agreement between Boltzmann and Monte Carlo rates agree to within 0.5%. We conclude from this excellent agreement that the Boltzmann treatment is valid in real experimental situations when boundaries are present and that the most accurate comparisons between the Boltzmann calculations and the excitation experiments will be for those experiments which focus on the center of the drift region rather than the entire drift distance.

SECTION IV

HIGH FIELD STRENGTHS

The extension of the method and the N_2 calculations presented, thus far, to higher values of E/N requires additional effort in two areas; development of the calculational method to include the new electron produced in the ionization events and the extension of the set of cross section data to higher energies with information on the differential scattering cross sections.

Rather than attempt to modify and extend the swarm derived cross sections used in Section III to higher energies, it was decided to review the literature and assemble the best possible set of cross sections, including the angular dependences relevant to our calculations. Because this cross section set has not been adjusted to yield calculated transport, excitation and ionization coefficients in agreement with experiment, this set should not be regarded as a recommended set for gas discharge laser, etc., calculations. This exercise was instructive in that it showed that while a large part of the necessary differential cross section data are available in the literature, there are some potentially important omissions and discrepancies.

1. Differential Scattering Cross Sections in N_2

The most convenient form of expressing the angular dependence of the cross sections for use in the multi-term Boltzmann code is as spherical harmonic components of the cross sections,

$$Q_i(\epsilon) = \int P_i(\cos \theta)Q(\theta, \epsilon)d\Omega ,$$

and, rather than entering the Q_i 's for all the cross sections in tabular form, it is easier to express the Q_i 's in terms of the Q_0 's, the total cross sections.

The angular dependences of the cross sections for elastic, rotational, vibrational, and electronic excitation and for ionization are presented in Table 1.¹⁸ The magnitudes of the cross sections were based¹⁸ on a previous swarm analysis¹⁹ for the low energy elastic and rotational cross sections, beam experiments for the higher energy elastic,²⁰ vibrational²¹ and electronic²² cross sections and on theory for the ionization cross sections.²³

2. Boltzmann Treatment of Ionization

For the higher values of E/N , the average electron energy is such that ionization becomes one of the most important, if not the dominant, inelastic energy loss channel. It is then necessary to include the new electrons produced in the ionization event in the calculation of the electron energy distribution functions. The mathematical model presented in Section II can include this effect and the appropriate equations are Eqs. (7) with a non-zero $\omega^{(0)}$,

$$\vec{a} \cdot \vec{\nabla}_{\vec{v}} f(\vec{v}) - \omega^{(0)} f(\vec{v}) = C[f'(\vec{v})] \quad (11)$$

where the collision term must be modified to include the scattering-in contribution of the new electron as is given, for example, by Thomas.²⁴

It is instructive at this point to write the Boltzmann equation explicitly. After the spherical harmonic expansion and subsequent projection of equations,⁵

$$\begin{aligned} & \frac{i}{2i-1} \left(\epsilon \frac{df_{i-1}(\epsilon)}{d\epsilon} - \frac{i-1}{2} f_{i-1}(\epsilon) \right) + \frac{i+1}{2i+3} \left(\epsilon \frac{df_{i+1}(\epsilon)}{d\epsilon} + \frac{i+2}{2} f_{i+1}(\epsilon) \right) \\ & + \frac{N}{E} \frac{v_i}{N} \epsilon^{1/2} f_i(\epsilon) = - \frac{N}{E} Q_T \epsilon f_i(\epsilon) + \frac{N}{E} 2 \frac{m}{n} \frac{d}{d\epsilon} (\epsilon^2 Q_m f_i(\epsilon)) \delta_{0,1} \\ & + \frac{N}{E} \sum_k (\epsilon + \epsilon_k) f_i(\epsilon + \epsilon_k) \int P_i(\cos \theta_s) Q_k(\cos \theta_s, \epsilon + \epsilon_k) d\Omega \\ & + I \quad \text{for } i = 0, \dots, N \end{aligned} \quad (12)$$

Table 1
RATIOS OF SPHERICAL HARMONIC COMPONENTS OF DIFFERENTIAL SCATTERING CROSS SECTIONS FOR N_2 USED IN BOLTZMANN EQUATION

Collision Process	Q_1/Q_0	Q_2/Q_0	Q_3/Q_0	Q_4/Q_0	Q_5/Q_0
Elastic Scattering	$\frac{1.2[(4.0\epsilon)^{1/2} + 0.4\epsilon]}{40 + (4.0\epsilon)^{1/2} + 0.4\epsilon} - \frac{0.2\epsilon^{1/2}}{0.025 + \epsilon^{1/2}}$	$\frac{0.84\epsilon}{20 + \epsilon} - \frac{0.04\epsilon}{0.01 + \epsilon} + \frac{0.2\epsilon}{3 \times 10^{-3} + \epsilon}$	$\frac{0.7\epsilon}{65 + \epsilon} + \frac{0.3\epsilon}{3000 + \epsilon}$	$\frac{0.61\epsilon^2}{2000 + \epsilon} + \frac{0.39\epsilon}{5000 + \epsilon}$	$\frac{0.55\epsilon^2}{4000 + \epsilon} + \frac{0.45\epsilon}{5000 + \epsilon}$
$A^3\Gamma_u^+, B^3\Pi, C^3\Delta$	$-\frac{\epsilon^2}{1500 + \epsilon^2}$	$-\frac{\epsilon^2}{10^4 + \epsilon^2}$	0	0	0
$B^3\Sigma_g^+, a^1\Sigma_g^+$	0	0	0	0	0
$W^1A_u, E^3\Sigma_g^+$	0	0	0	0	0
One electron from ionization					
$c^3\Pi$	-0.2	0	0	0	0
$a^1\Pi_g$	$\frac{80}{80 + \epsilon^2} + \frac{\epsilon^2}{2500 + \epsilon^2}$	$\frac{\epsilon^2}{1600 + \epsilon^2}$	$\frac{\epsilon^2}{3500 + \epsilon^2}$	$\frac{\epsilon^2}{3500 + \epsilon^2}$	$\frac{\epsilon^2}{3500 + \epsilon^2}$
"Sum of singlets" One electron from ionization					
V Vibrational excitation (all levels)	0	0	0	0	0
R Resonant rotational excitation	0	0	0	0	0

where Q_T is the total cross section, Q_m is the elastic momentum transfer cross section, Q_k is the i th inelastic cross section, ε_k is the threshold energy of the k th inelastic process, ν_i is the ionization frequency, and I is defined later. ν_i as used here equals $\omega^{(0)}$ in Eq. (5) and is the exponential growth constant of the total number of electrons in the gap in a pulsed Townsend type experiment as discussed by Thomas.²⁴ The first term on the right represents electrons scattered out of an energy element $d\varepsilon$ centered about ε due to all collisions. The second term on the right represents electrons scattered into $d\varepsilon$ from all elements $d\varepsilon^+$ centered about ε^+ that are connected to $d\varepsilon$ by inelastic collisions.

When ionization is included, the scattering-out term does not change. The contribution of ionization to the scattering-out term is independent of any electron production. However, the new electron will contribute a scattering-in component. We assume that the primary and secondary electrons share the excess energy of the primary over the ionization threshold, ε_i , in a ratio $q:1-q$ where $0 < q < 1$. Then in order for the primary to scatter into $d\varepsilon$ it must start with an energy $\varepsilon^+ = (\varepsilon/q) + \varepsilon_i$ before the collision. Similarly, for the secondary to scatter into $d\varepsilon$ it must have originated in an ionization collision between a neutral and a primary electron of energy $\varepsilon^+ = [\varepsilon/(1-q)] + \varepsilon_i$. Since the rate of events leading to the scattering-in of electrons into an element $d\varepsilon$ centered about ε is $\varepsilon^+ N Q(\varepsilon^+) f(\varepsilon^+)$, the scattering-in contribution from ionization considering the secondary electron production is,

$$I = \frac{1}{q} \left(\frac{\varepsilon}{q} + \varepsilon_i \right) N f \left(\frac{\varepsilon}{q} + \varepsilon_i \right) Q \left(\frac{\varepsilon}{q} + \varepsilon_i \right) + \frac{1}{(1-q)} \left(\frac{\varepsilon}{(1-q)} + \varepsilon_i \right) N f \left(\frac{\varepsilon}{(1-q)} + \varepsilon_i \right) Q \left(\frac{\varepsilon}{(1-q)} + \varepsilon_i \right) . \quad (13)$$

Rigorously, q is a function of ϵ . However, the work of Tagashira²⁵ and of Hayashi²⁶ suggests that setting $q = 1/2$ at all energies is a good approximation. We have, therefore, used $q = 1/2$ in all the following calculations to reduce the variation of parameter space.

3. Numerical Results Considering Ionization

The effect of ionization is not significant for E/N less than about 200 Td because below that value, less than 3% of the electron energy loss is due to ionization. We carried out calculations including ionization at 300, 500, 1000 and 2000 Td and compare to calculations where ionization is treated as an energy loss only. These calculations are based on the cross sections presented in paragraph 1 of Section IV but using isotropic cross sections only in order to isolate the effect of ionization.

It can be seen in Eqs. (12) and (13) that the inclusion of the secondary electrons produced in the ionization event adds a term dependent on v_i/N and changes the form of the ionization scattering-in contribution in the collision operator. The sign of the v_i/N term and the dependence on f is the same as that of the scattering-out contribution in the collision operator. Therefore, when this term is included, it appears that the scattering-out has increased. The ionization modified scattering-in must balance this additional scattering-out-like effect. The overall effect is a shift of the distribution to lower energies because the scattering-in electrons come in at lower energies.

The solutions of Eqs. (12) were carried out iteratively because v_i/N is a function of the distribution function, f . It was possible to find a consistent solution; i.e., a solution where the input value and the calculated value of v_i/N were equal, by straightforward iteration. However, a more efficient way to arrive at a consistent solution was to calculate the energy balance.¹⁹ We

define the energy balance as the ratio of the power gained by the electrons due to the field, FPG, to the power lost in collisions, CPL. In a consistent solution, this ratio should be unity. Departures from unity are due to an inconsistent value of v_i/N and it is possible to use the energy balance to guide the iteration. We write

$$FPG = CPL + IPL$$

where IPL is the ionization power lost and note that we have shown that

$$IPL = (\langle \epsilon \rangle + \epsilon_i) v_i ,$$

where $\langle \epsilon \rangle$ is the average electron energy. The energy balance is

$$EB = \frac{FPG}{CPL + IPL} = \frac{FPG}{CPL + (\langle \epsilon \rangle + \epsilon_i) v_i} . \quad (14)$$

While it is not possible to obtain a new value of v_i from this relation, Eq. (14) does provide a good guide to the selection of the next v_i value. If EB is less than (greater than) one, v_i is too large (small). With some practice, the number of iterations can be reduced to two or three.

Calculations at these higher E/N values are done with three approximations, two-term without ionization, and two- and six-terms with ionization. Based on the convergence studies shown in Section II, we assumed that the calculations at these E/N had converged with six terms in the spherical harmonic expansion. Several quick checks were made at 500 and 1000 Td which confirmed this assumption. Values of the drift velocity, W , transverse diffusion coefficient, D_T , normalized ionization frequency, v_i/N , as well as fractional ionization power lost are shown in Table 2 for four values of E/N. The results are much as expected. We see by comparison of the two-term solutions with and without ionization that the distribution is shifted towards lower energies

Table 2
THE EFFECT OF INCLUDING THE ELECTRON PRODUCTION DURING
IONIZATION ON CALCULATED TRANSPORT PARAMETERS IN N_2

	Two-term (No ionization)	Two-term (Ionization)	Six-term (Ionization)
300 Td			
W ($\times 10^7$ cm sec $^{-1}$)	2.335	2.342	2.319
D _T N ($\times 10^{22}$ cm $^{-1}$ sec $^{-1}$)	3.85	3.83	3.440
v _i /N ($\times 10^{-9}$ cm 3 sec $^{-1}$)	0.200	0.197	0.219
$\langle \epsilon \rangle$ (eV)	6.54	6.49	6.44
% ϵ -loss to ionization	4.42	4.42	4.97
500 Td			
W ($\times 10^7$ cm sec $^{-1}$)	3.308	3.347	3.306
D _T N ($\times 10^{22}$ cm $^{-1}$ sec $^{-1}$)	4.51	4.44	3.85
v _i /N ($\times 10^{-9}$ cm 3 sec $^{-1}$)	1.38	1.20	1.22
$\langle \epsilon \rangle$ (eV)	9.11	8.84	8.70
% ϵ -loss to ionization	12.89	11.96	12.47
1000 Td			
W ($\times 10^7$ cm sec $^{-1}$)	5.118	5.255	5.158
D _T N ($\times 10^{22}$ cm $^{-1}$ sec $^{-1}$)	5.98	5.62	4.49
v _i /N ($\times 10^{-9}$ cm 3 sec $^{-1}$)	10.25	7.49	7.53
$\langle \epsilon \rangle$ (eV)	16.16	14.36	14.16
% ϵ -loss to ionization	31.04	27.66	28.41
2000 Td			
W ($\times 10^7$ cm sec $^{-1}$)	7.770	8.139	7.942
D _T N ($\times 10^{22}$ cm $^{-1}$ sec $^{-1}$)	10.89	7.76	5.599
v _i /N ($\times 10^{-9}$ cm 3 sec $^{-1}$)	51.64	26.5	26.10
$\langle \epsilon \rangle$ (eV)	41.53	25.40	25.88
% ϵ -loss to ionization	51.96	42.83	43.20

with the inclusion of ionization. The effect of more terms in the expansion is to shift the distribution function towards higher energies and bring the results slightly back toward the two-term values without ionization. Very large effects appear in the diffusion coefficients and this is due to the increase in the spatial gradients when ionization is present. The spatial dependence is included as discussed in Section II.

We see then that the inclusion of ionization is critical to an accurate calculation of swarm parameters at high E/N . The error introduced by the two-term approximation is dwarfed in comparison except in the case of diffusion. There, the two-term approximation is more severe than the neglect of ionization.

4. Anisotropic Scattering Effects

As mentioned above, anisotropies in the cross sections up to the order of the Legendre functions retained in the expansion of the distribution function may be included in the multi-term Boltzmann formulation. That this is the case can be seen from the collision operator;

$$NQ_T(\varepsilon)\varepsilon f_i(\varepsilon) - N \sum_k (\varepsilon + \varepsilon_k) f_i(\varepsilon + \varepsilon_k) \int Q_k(\varepsilon + \varepsilon_k, \theta) P_i(\cos \theta) d\Omega$$

for $i = 0, \dots, N$.

The integral in the scattering-in term picks out only the i th Legendre component of the cross section. For example, in the two-term expansion the momentum transfer cross section comes up because it contains the isotropic and the $\cos \theta$ components of the differential cross sections, the same angular components included in the two-term distribution function. In the multi-term analysis, a convenient form for representing the angular distribution of the cross sections is

$$Q_i(\varepsilon) = \int Q(\varepsilon, \theta) P_i(\cos \theta) d\Omega .$$

We first calculated the distribution function and the associated swarm parameters from 1 to 200 Td for average electron energies from 0.3 to 4.5 eV with the anisotropies in the elastic and vibrational cross sections given in this section. The neglect of anisotropies in the electronic excitation cross sections is well justified for $E/N \lesssim 100$ Td when only a small fraction of the electron energy goes into the electronic channels but probably not a very good assumption at 200 Td. We find that for these cross sections, there is little or no difference in the calculations of the measurable parameters from 1 to 200 Td.

In order to compare the calculations with and without these anisotropies, it is necessary to determine what to keep constant between the calculations. We have kept the elastic momentum transfer constant and in so doing, the f_0 and f_1 equations differ only by virtue of $\cos \theta$ components in the inelastic cross sections. Because the vibrational anisotropies do not include a $\cos \theta$ component, the two-term with and two-term without anisotropies are identical for the 1-200 Td calculations.

For higher values of E/N with the correspondingly higher average electron energies, the anisotropies in the cross sections become more pronounced and potentially more important in the calculations. We have calculated the distribution function and the swarm parameters at 500 Td where the average electron energy is about 8.8 eV using the full set of differential cross sections shown in Table 3.

Table 3 shows our results with four approximations, the two-term without anisotropies and the two-, four- and six-term with the anisotropies. Ionization is included in all four cases. For these calculations, the elastic momentum transfer was again kept constant. The only difference between the two-term with and the two-term without anisotropies is then due to a different inelastic momentum transfer. The overall effect of the addition of anisotropies is to

Table 3

THE EFFECT OF ANISOTROPIC SCATTERING ON THE CALCULATED VALUES OF
TRANSPORT AND RATE COEFFICIENTS AT 500 Td

	Two-term Isotropic	Two-term Anisotropic	Four-term Anisotropic	Six-term Anisotropic
W ($\times 10^7$ cm sec $^{-1}$)	3.35	3.54	3.32	3.31
D_T^N ($\times 10^{22}$ cm $^{-1}$ sec $^{-1}$)	4.44	3.40	2.98	3.01
A state ($\times 10^{-9}$ cm 3 sec $^{-1}$)	1.59	1.59	1.53	1.53
C state ($\times 10^{-9}$ cm 3 sec $^{-1}$)	1.75	1.75	1.67	1.67
Ionization ($\times 10^{-9}$ cm 3 sec $^{-1}$)	1.20	1.13	1.16	1.26
$\langle \epsilon \rangle$ (eV)	8.84	8.86	8.66	8.72

shift the distribution towards higher energies. This is to be expected if the anisotropies are primarily in the forward direction as the directed velocities tend to be preserved in the anisotropic case and destroyed in the isotropic case. The effect of higher order expansion coefficients as seen in the comparison of the two- and six-term results with anisotropies is different from the isotropic case and will depend on the particular differential cross sections involved. The effect of anisotropies in Eqs. (12) is to add scattering-in terms in the higher order equations. Whereas, before the only source of the higher order coefficients, the f_i 's, was due to the field, we now have scattering-in contributions to those coefficients.

The preliminary conclusion drawn from these examples is that when the electron energies are such that an appreciable number of the electron-neutral collisions are anisotropic, the effect must be included, and the number of terms in the expansion must be high enough so that the anisotropies can be well represented by the same order expansion of the cross sections. A more complete investigation of the effect of anisotropies at high E/N would be desirable.

SECTION V

CONCLUSIONS

The original purpose of this work was to develop a method of solving the Boltzmann equation suitable for the extraction of cross sections from swarm experiments for cases where the usual two-term approximation was of questionable validity. The criteria for the validity of the two-term approximation are low field strengths and small ratio of inelastic to elastic cross sections.^{3a} An arbitrary ratio of inelastic to elastic cross sections can be accommodated with the multi-term method and the high field cases can be treated when proper account is made of electron production during ionization and anisotropies in the scattering cross sections. The extension of the Boltzmann analysis from a two-term to a multi-term spherical harmonic expansion method was accomplished last year under this contract and a detailed description may be found in Reference 5. A summary is presented in Section II.

This year we have made a study of the convergence properties of the Boltzmann solution and calculated swarm parameters in the case of N_2 at moderate field strengths (1-200 Td). The error introduced by the two-term approximation is small (~1%) for drift velocities, larger for the diffusion coefficients (~5%) and even larger for the excitation rates, 30% in the worst cases. The maximum error occurred at an E/N of 70 Td, where the electrons are "seeing" the largest ratio of inelastic to elastic cross sections. Convergence of the transport and excitation coefficients with a number of terms in the expansion to within a few percent was achieved by four terms in all cases. These errors are significant for the extraction of cross sections from swarm experiments if those cross sections are to be compared, for example, with beam data. If, however, two-term derived cross sections are used in a two-term calculation

of swarm parameters, these errors may be tolerable in applications other than cross section determinations.

Effects of electron production in ionization and anisotropic electron scattering must be considered in high field calculations. The division between moderate and high fields here is based on the amount of electron energy lost in ionization. E/N values greater than 200 Td in N_2 , at which point 3% of the electron energy goes into ionization, are considered high fields. The inclusion of electron production into the Boltzmann formulation is straightforward but the resulting equations must be solved iteratively. With experience, the number of iterations is small. The results of Section IV show that the neglect of electron production is more severe than the two-term approximation at high E/N .

Anisotropic scattering is potentially very important at high E/N but negligible for low E/N with the anisotropies given in Table 1. Anisotropies in the cross sections introduce scattering-in sources in the higher order equations for the distribution function. The issue of convergence then has two aspects, convergence of the spherical harmonic series representation of the differential cross sections as well as of the distribution function. In contrast to the low E/N calculations, the effect of anisotropies in N_2 at 500 Td is quite significant.

Superelastic effects are included in the multi-term Boltzmann formulation, but sufficient data have not been compiled at this time for cross sections from excited vibrational levels, for example, to make an investigation of the effects worthwhile.

In summary, the calculations of electron transport and rate parameters using the multi-term Boltzmann method can be made as accurate as required for the iterative extraction of cross sections from swarm experiments over a wide

range of field strengths corresponding to a nearly thermal distribution at one end and a distribution markedly affected by electron production in ionization at the other.

REFERENCES

1. B. Bederson and L. J. Kieffer, *Rev. Mod. Phys.* 43, 601 (1971).
2. a) L. S. Frost and A. V. Phelps, *Phys. Rev.* 127, 1621 (1962); b) H. B. Milloy and R. W. Crompton, *Phys. Rev. A* 15, 1847 (1977); c) P. Kleban and H. T. Davis, *J. Chem. Phys.* 68, 2999 (1978); d) K. Kitamori, H. Tagashira and Y. Sakai, *J. Phys. D* 11, 283 (1978); e) T. Makabe and T. Mori, *J. Phys. (Paris) Colloq.* 40, 43 (1979); f) S. L. Lin, R. E. Robson and E. A. Mason, *J. Chem. Phys.* 71, 3483 (1979).
3. a) T. Holstein, *Phys. Rev.* 70, 367 (1946); b) W. P. Allis, in Handbuch der Physik, edited by S. Flügge (Springer, Berlin, 1956), Vol. 21, pp. 383-444.
4. a) P. E. Luft, JILA Information Center Report No. 14, October, 1975; b) W. L. Morgan, JILA Information Center Report No. 19, June, 1979; c) S. D. Rockwood, *Phys. Rev. A* 8, 2348 (1973); d) C. J. Elliot and A. E. Greene, *J. Appl. Phys.* 47, 2946 (1976); e) W. L. Nighan, *Phys. Rev. A* 2, 1989 (1970).
5. L. C. Pitchford, S. V. O'Neil and J. R. Rumble, Jr., *Phys. Rev. A* (to appear). The sign of \vec{a} has been changed in this report. Here $\vec{a} = e\vec{E}/m$.
6. L. C. Pitchford and E. C. Beaty, Technical Report AFWAL-TR-80-2019, March, 1980.
7. A. V. Phelps, D. Levron and K. Tachibana, in Proceedings of the XIth International Conference on the Physics of Electronic and Atomic Collisions, edited by K. Takayanagi and N. Oda (Kyoto, 1979), p. 318.
8. J. H. Parker, Jr. and J. J. Lowke, *Phys. Rev.* 181, 290 (1969).
9. H. R. Skullerud, in Proceedings of the XIIIth International Conference on Phenomena in Ionized Gases, part III, *Phys. Soc. G.D.R. (Berlin*, 1977).
10. B. Sherman, *J. Math. Anal. and Appl.* 1, 342 (1960).

11. C. de Boor, *J. Approx. Theory* 6, 50 (1972).
12. N. L. Schryer, *Bell Laboratories Computing Science Technical Report No. 52*, 1976 (unpublished).
13. The Monte Carlo code used in the calculations reported here is originally due to I. Reid and is described in his thesis, *Australian National University*, 1978.
14. W. P. Allis, private communication.
15. K. Tachibana and A. V. Phelps, *J. Chem. Phys.* 71, 3544 (1978); D. Levron and A. V. Phelps, *J. Chem. Phys.* 69, 2260 (1978).
16. V. V. Urosević, Z. Lj. Petrović, J. V. Bozin, Lj. D. Zeković, in Proceedings of the Summer School and Symposium on the Physics of Ionized Gases, edited by B. Cobić (Dubrovnik, Yugoslavia, 1980).
17. J. J. Lowke and D. K. Davies, *J. Appl. Phys.* 48, 4991 (1978).
18. A. V. Phelps, private communication.
19. A. G. Engelhardt, A. V. Phelps and C. G. Risk, *Phys. Rev.* 135, 1566 (1964).
20. J. P. Bromberg, *J. Chem. Phys.* 52, 1243 (1970); R. H. J. Jansen, F. J. de Heer, H. J. Luyken, B. van Wingerden and H. J. Blaauw, *J. Phys. B* 9, 185 (1976); S. K. Srivastava, A. Chutjian and S. Trajmar, *J. Chem. Phys.* 64, 1340 (1976); R. D. du Bois and M. E. Rudd, *J. Phys. B* 9, 2657 (1976).
21. G. J. Schulz, *Phys. Rev.* 135, A983 (1964).
22. D. C. Cartwright, S. Trajmar, A. Chutjian and W. Williams, *Phys. Rev. A* 16, 1041 (1977).
23. D. Rapp and P. Englander-Golden, *J. Chem. Phys.* 43, 1464 (1965).
24. W. R. L. Thomas, *J. Phys. B* 2, 551 (1969).
25. H. Tagashira, private communication.
26. M. Hayashi, private communication.